

Theory of the peroxy-radical defect in  $\alpha$ -SiO<sub>2</sub>

Arthur H. Edwards and W. Beall Fowler

*Department of Physics and Sherman Fairchild Laboratory, Lehigh University,  
Bethlehem, Pennsylvania 18015*

(Received 22 June 1982)

We have investigated the peroxy-radical defect in glassy SiO<sub>2</sub> by means of MOPN, a semi-empirical molecular-orbital program, applied to a cluster of atoms chosen to simulate the defect. Our calculations are consistent with important features of Griscom's model of the defect as a perturbed O<sub>2</sub><sup>-</sup> ion substituted for a single-bridging O<sup>2-</sup> ion in SiO<sub>2</sub> and attached to a *single* silicon, and they place geometrical constraints on the defect structure for this model to be valid. We predict the existence of a related defect (the small peroxy radical, or SPR) wherein the peroxy radical is strongly bonded to *two* silicons. We have also investigated the formation of the peroxy radical. Griscom and co-workers envision peroxy linkages substituting for single-bridging oxygens during the growth process. They suggest that upon annealing these linkages readily give up an electron to form the observed radical. Our calculations lead us to argue against this process; rather, capture of a free hole seems more likely. We suggest that the SPR could form via a process in which neutral oxygen molecules diffuse through the solid and combine with E'<sub>1</sub> centers to form peroxy radicals.

## I. INTRODUCTION

Griscom, Friebele, and co-workers recently completed a set of detailed studies of the electron-paramagnetic-resonance (EPR) spectra of high-purity (less than 1-ppm foreign cations) wet and dry fused silica.<sup>1-5</sup> Their experiments were performed on isotopically enriched samples and combined optical and EPR spectroscopy with isochronal pulse annealing techniques. From these studies, detailed microscopic models emerged for three fundamental defects, the E' center,<sup>4,5</sup> the nonbridging oxygen hole center (NBOHC),<sup>1,3</sup> and the peroxy radical<sup>1,3</sup> (PR). Models for these defects are shown in Fig. 1.

The E' center is an oxygen vacancy with a hole trapped primarily on one of the silicon atoms nearest the vacancy. The unpaired electron remaining on the other silicon is EPR-active. The NBOHC, as its name implies, is a trapped hole on a singly coordinated O<sup>2-</sup> ion.<sup>6</sup> The peroxy radical is a trapped hole on a singly coordinated O<sub>2</sub><sup>2-</sup> molecule ion. These descriptions, though stated as fact, are models, and only one of these models (the E'<sub>1</sub> center in  $\alpha$ -quartz) has been previously tested theoretically.<sup>7</sup> There is, however, a large body of experimental evidence, discussed below, that renders most of the details of the models unambiguous.

Griscom and co-workers paid particular attention to the annealing and radiation behavior of these defects.<sup>1</sup> The peroxy radical exhibits surprising behavior in that, for temperatures below about 400°C, the concentration of this defect grows with annealing temperature and with radiation dose, while in the same temperature range the concentrations of NBOHC and E' centers decrease. Griscom<sup>1,2</sup> has suggested, as a model for the defect precursor, peroxy linkages grown into the oxide. To account for the annealing data Griscom suggested that such stable linkages could easily shed an electron, leading to formation of the peroxy-radical center.

In this paper we present the first detailed theoretical treatment of the peroxy radical.<sup>8</sup> In Sec. II we review the experimental results and the proposed model for the peroxy radical. Because some con-

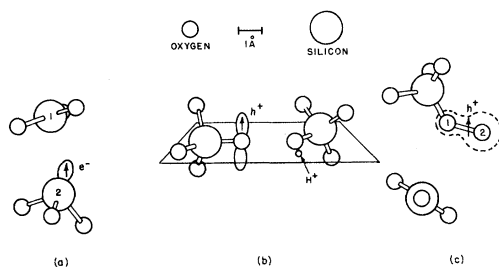


FIG. 1. Models for three fundamental defects in SiO<sub>2</sub>: (a) E'<sub>1</sub> center in  $\alpha$ -quartz. The hole is trapped on silicon 1, while the unpaired electron is on silicon 2 (Ref. 7). A similar model is thought to be valid in fused silica. (b) NBOHC in fused silica [after D. L. Griscom, *J. Non-Cryst. Solids* **31**, 241 (1979)]. (c) Peroxy radical (PR) in fused silica (Ref. 3).

clusions about this defect depend on the results for the NBOHC and  $E'$  centers, we include discussions of these where necessary.

In Sec. III we briefly discuss MINDO/3, the molecular-orbital method used for the calculations. This is planned to be discussed in detail elsewhere,<sup>9</sup> as will our results for bulk SiO<sub>2</sub> and other well-understood defects. These results indicate that MINDO/3 gives a remarkably reliable picture of SiO<sub>2</sub>.

In Sec. IV we present our results for the peroxy radical (PR) and its precursor. We develop two models for the peroxy radical. In one, the peroxy radical is attached to a single silicon atom,<sup>1-3</sup> and the unattached silicon atom relaxes into the plane of its remaining three oxygen neighbors. We argue that this model (the PR model) is appropriate for situations in which there are large Si-Si separations. In the second model, the peroxy radical is strongly bonded to two silicon atoms, but only one of the two oxygen atoms of the peroxy radical is involved in this bonding. Because this model apparently would be appropriate for normal Si-Si separations (between  $\sim 3.05$  and  $3.25$  Å), we call it the small peroxy radical (SPR). While both of these models are consistent with <sup>17</sup>O hyperfine data, only the PR exhibits the appropriate <sup>29</sup>Si hyperfine interaction<sup>3</sup>, and to date there is no experimental evidence for the existence of the SPR. This is discussed in detail in Secs. II and IV.

The defect-formation problem has been considered for both of these models. For normal Si-Si separations, our calculations indicate that a peroxy-linkage precursor would be energetically unfavored by about 3 eV. We infer from this energy difference that such precursors are unlikely to occur in the growth process of crystalline SiO<sub>2</sub>. Formation of the SPR *could*, however, take place by a mechanism in which dissolved O<sub>2</sub> molecules diffuse and combine with existing  $E'$  centers.

In the case of large Si-Si separations, the peroxy linkage is favored energetically over a single-bridging oxygen atom. However, the annealing behavior is not in agreement with our calculations at this point in that we do not predict that the precursor will readily "shed" an electron. We suggest, rather, that hole trapping is responsible for creation of the peroxy radical. This is discussed further in Sec. V.

## II. EXPERIMENTAL BACKGROUND

The first EPR spectra of neutron-irradiated crystalline and fused quartz were obtained by Weeks<sup>10</sup>

over 20 years ago. The spectra of both materials consisted of a single sharp line and a broad absorption band, the band in the crystal showing more structure. Further experiments by Silsbee<sup>11</sup> on crystalline  $\alpha$ -quartz indicated that the sharp line had hyperfine satellites that were weak in intensity, but whose splittings were indicative of both strong and weak interactions.

Detailed analysis<sup>7</sup> of these lines led to the model for the  $E'_1$  center shown in Fig. 1(a). Theoretical calculations<sup>7</sup> using this model have reproduced most experimental results. We plan to discuss these results in detail elsewhere.<sup>9</sup>

While the  $E'$  resonance data received a good deal of attention in the literature,<sup>10-13</sup> the broad EPR absorption accompanying the  $E'$  signal was almost ignored. It was known to have very weak <sup>29</sup>Si hyperfine interaction,<sup>13</sup> indicating that the spin was associated with the oxygen sublattice. The  $g$  shifts implied that the spin was probably a hole.<sup>10</sup>

Recently Griscom and co-workers have undertaken a detailed study of this spectrum in noncrystalline SiO<sub>2</sub>. Through isochronal pulse annealing studies on both "wet" (high OH content) and "dry" (low OH content) silicas, Friebele *et al.*<sup>14</sup> determined that the broad band was a superposition of signals due to two different defects. One of these is predominant in wet oxides and the other in dry. Further identification was facilitated by enriching samples<sup>1</sup> with <sup>17</sup>O. The <sup>17</sup>O hyperfine data indicated that the oxygen-related hole center (OHC) in wet silica was a hole trapped on a single oxygen atom in a lone-pair  $p$  orbital.

The final model<sup>1</sup> for the OHC in wet silica, shown in Fig. 1(b), has the nonbridging oxygen atom facing an OH group. The presence of the OH group is consistent with the strong positive correlation of the amplitude of the NBOHC (wet OHC) EPR signal with the number density of OH groups in the glass, and with thermodynamic calculations.<sup>15</sup>

The OHC in dry silica has also been analyzed<sup>1</sup> using <sup>17</sup>O-enriched samples. The dry oxides were enriched to 36 at. % <sup>17</sup>O and then annealed at 550°C. This treatment eliminated the  $E'$  center while it maximized the ratio of dry to wet OHC concentrations. A successful computer simulation of the resulting EPR spectrum was obtained<sup>1</sup> by using the following assumptions:

- (1) The spin is associated with a perturbed O<sub>2</sub><sup>-</sup> ion which is assumed to be configured as in Fig. 1(c).
- (2) Given the 36-at. % <sup>17</sup>O enrichment, the possi-

ble combinations of <sup>16</sup>O, <sup>17</sup>O could be obtained for the two oxygen sites. The appropriate weighting factors for each configuration were calculated, along with the number of EPR lines expected.

(3) The value for  $g_3$  was obtained from a best fit to the experimental spectrum.  $g_1$  and  $g_2$  were obtained from the theory of the O<sub>2</sub><sup>-</sup> ion.<sup>16</sup>

(4) The values for the hyperfine parameters  $A_{||}$  and  $A_{\perp}$  were also obtained from best fits to experiment with the assumption that 100% of the spin resided on the two oxygen atoms.

From the computer simulation of the EPR spectrum it was determined that the spin has almost pure  $p$  character, and that it spends 74% of its time on one oxygen atom and 26% on the other. Although it was impossible to determine on which oxygen the spin spends most of its time, it was assumed to be primarily on the terminating oxygen in Fig. 1(c).

Isochronal pulse annealing studies have also been performed on the dry oxides<sup>1</sup>. In these experiments the irradiated sample was subjected to a series of 10-min annealing steps. In each successive step, the temperature was increased by 50°C. Between steps the sample was cooled to 77 K for EPR measurements and then allowed to warm up to room temperature for optical-absorption measurements. The results of these experiments are shown in Fig. 2.

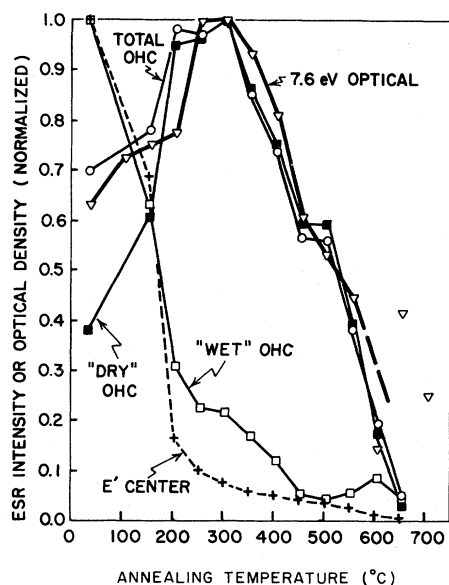


FIG. 2. Correlation of the intensity of the EPR spectra of the "wet," "dry," and total (wet + dry) oxygen-associated hole centers in  $\gamma$ -irradiated Suprasil W-1 with the peak height of the 7.6-eV optical-absorption band as a function of 10-min isochronal anneals (after Ref. 1).

Note that the  $E'$  and the NBOHC (wet OHC) EPR signals decrease monotonically with increasing annealing temperature, while the dry OHC signal increases with temperature up to 350°C. Note also that the 7.6-eV optical absorption also rises, indicating that it is probably associated only with the dry OHC.

To account for the <sup>17</sup>O hyperfine data, along with the optical correlation and annealing characteristics, Griscom and co-workers proposed the following model.<sup>1,2</sup> Pre-existing in the glass are Si-O-O-Si linkages, wherein O<sub>2</sub><sup>2-</sup> molecules substitute for O<sup>2-</sup> ions.<sup>6</sup> These molecules are assumed to be precursors of the peroxy radical. It is argued that upon radiation or annealing, this linkage readily gives up an electron, breaking an Si-O bond, and forming the configuration shown in Fig. 1(c). At the same time, the silicon that is only threefold coordinated relaxes in a manner similar to the  $E'_1$  center. The assertion that this system should easily shed an electron is made on the strength of experiments on peroxy-borate glasses.<sup>17</sup>

Griscom and Friebele recently completed a set of EPR experiments on dry, <sup>29</sup>Si-enriched oxides.<sup>3</sup> The changes in the EPR spectra due to enriching the sample with <sup>29</sup>Si are indicative of a strong hyperfine interaction with a *single* silicon atom. To within experimental resolution, the evidence is strongest for a conformation in which the peroxy radical is attached to only a single silicon atom. In fact, the experiment indicates that the unpaired spin interacts at least 5 times more intensely with one silicon than with any other.

Also, the <sup>29</sup>Si hyperfine parameters  $A_1$  and  $A_2$  obtained from the computer simulation indicate that the hyperfine splittings for the peroxy radical are 30% of those exhibited by the nonbridging oxygen hole center.<sup>3</sup> If it is assumed that the hyperfine splitting is due to interaction of the <sup>29</sup>Si nucleus with only the site-1 oxygen (a reasonable assumption in light of the strong distance dependence of the hyperfine interaction), this lends support to the contention that most of the hole spin density resides on the far oxygen atom, site 2.

Finally, it is argued by Griscom and Friebele<sup>3</sup> that the inequality of  $A_1$  and  $A_2$  for the peroxy radical indicates that the Si-O-O bond angle is less than 180°.

### III. THEORETICAL BACKGROUND

We used a semiempirical linear combination of atomic orbitals and molecular-orbital (LCAO-MO)

program MOPN (Ref. 18) to obtain molecular orbitals, total energies, and spin densities for a small cluster (shown in Fig. 3) that was used to represent the peroxy radical in  $\text{SiO}_2$ . This cluster consists of two Si, eight O, and six H; the H atoms are used to terminate possible dangling bonds.

MOPN, an unrestricted Hartree-Fock version of MINDO/3,<sup>19</sup> is based on the intermediate neglect of differential overlap (INDO) approximation. If  $\varphi_{iA}(\vec{r})$  is the basis set of atomic valence orbitals, where  $i$  labels the atom and  $A$  is the set of atomic quantum numbers, then in the complete neglect of differential overlap (NDO) approximation,

$$\varphi_{iA}(\vec{r})\varphi_{jB}(\vec{r})=0, \quad i \neq j, \quad A \neq B.$$

This approximation eliminates all three- and four-center and most two-center matrix elements. It also eliminates all exchange integrals and hence will give no term splitting. INDO ameliorates this deficiency by including all one-center, two-electron matrix elements. The remaining one- and two-center integrals are either parametrized or evaluated using empirical formulas.<sup>9,19</sup> The parameters are fit to obtain good agreement with experimental molecular heats of formation, bond lengths, and bond energies.

As a result, MINDO/3 gives remarkably accurate predictions for conformations of molecules and point defects,<sup>9,20</sup> with a few notable exceptions.<sup>21-23</sup>

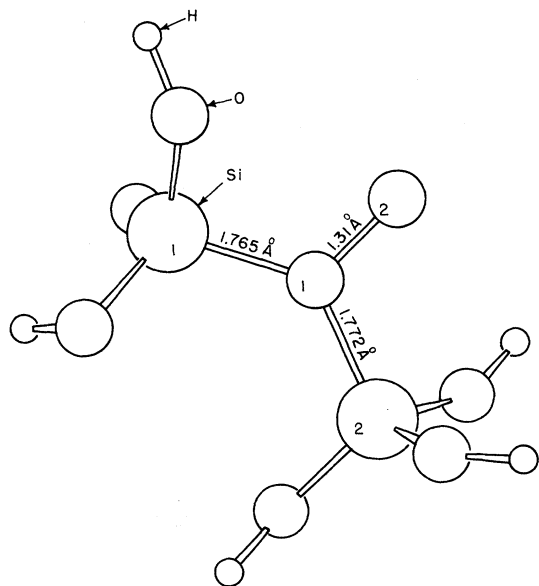


FIG. 3. Minimum energy conformation for the peroxy radical with outer oxygens at  $\alpha$ -quartz positions (i.e., the SPR) as computed by MOPN. This also illustrates the cluster of atoms used in all of our calculations.

An important failure of MINDO/3 is that it consistently predicts bond angles larger than experiment for heavy atoms.<sup>21,22</sup> This has specific importance to our calculations in  $\text{SiO}_2$ . MINDO/3 and most other NDO methods predict that the Si—O—Si bond angle will be linear, while the experimental value is  $\sim 144^\circ$ . Even in  $\text{Si}_2\text{OH}_6$ , disiloxane, the Si—O—Si angle is about  $140^\circ$ . This failure forced us to use various constraints to ensure nonlinear Si—O—Si bond angles. In most calculations we fixed the positions of the six outer oxygen atoms (Fig. 3). This technique gave good results for calculations on  $E'$  centers.<sup>9</sup>

MINDO/3 and MOPN contain routines that automatically search for minima in total energy with respect to molecular geometry. This is an extremely important feature for calculations such as ours.

## IV. CALCULATIONS AND DISCUSSION

### A. The peroxy radical

Considering the cluster shown in Fig. 3, we investigated the effects of a wide range of geometrical constraints on the results of calculations using MOPN. From these calculations two models for the peroxy radical emerged. In the first model, the site-1 oxygen is bonded to two silicon atoms as shown in Fig. 3. This model resulted from calculations in which the Si-Si separation was constrained to be between 3.05 and 3.24 Å. In the second model, appropriate for very large Si-Si separations, we obtained results that were in good agreement with Griscom's prediction.

While both of these models agree with the  $^{17}\text{O}$  hyperfine data, the first model (the SPR) has been ruled out as the observed peroxy radical in fused silica by a combination of Griscom's  $^{29}\text{Si}$  hyperfine data<sup>3</sup> and by our own hyperfine calculations. However, there appears to be no *a priori* reason why the SPR should not exist, particularly in crystalline  $\text{SiO}_2$ , and for this reason a discussion of the SPR is included here.

In our first calculations on the SPR the outer oxygen atoms were fixed in the normal  $\alpha$ -quartz positions. From neutron and x-ray scattering studies of amorphous  $\text{SiO}_2$  and most crystalline forms<sup>24,25</sup> of  $\text{SiO}_2$ , this seems a reasonable local geometry. The terminating hydrogen atoms were attached with O—H bond lengths of 0.93 Å and Si—O—H bond angles of  $144^\circ$ .

The cluster was given a net positive charge ( $+e$ ) to simulate the radical, and the two central oxygen

atoms and the two silicon atoms were allowed to search for positions of minimum total energy. Figure 3 is in fact obtained from an ORTEP (Ref. 26) plot with atomic positions that minimize total energy for the SPR case.

Many of the features of this predicted defect are the same as for the observed peroxy defect, with the exception of the <sup>29</sup>Si data. In particular, the O<sub>1</sub>-O<sub>2</sub> distance is 1.31 Å, close to the experimental value for the bond length<sup>27</sup> for free O<sub>2</sub><sup>-</sup>, and to the MOPN prediction for free O<sub>2</sub><sup>-</sup>. The *p*-spin density displays the correct asymmetry, as shown in Table I.

The predicted silicon *s*-spin density is shown in Table II. These values lead to a 12:7 ratio between the hyperfine interactions with Si<sub>1</sub> and Si<sub>2</sub>. This inequality is somewhat surprising, considering the near equivalence of the Si<sub>1</sub>-O<sub>1</sub> and Si<sub>2</sub>-O<sub>1</sub> bond-lengths. It points up the fact that the two silicons are not equivalent when all the atoms in the cluster (or solid) are taken into account.

The computed one-electron spectrum of the SPR is shown in Fig. 4. Below the dashed line indicated as the Fermi level, there are 31 "α" spin-occupied states and 30 "β" spin-occupied states. There is an extra β-spin virtual orbital, indicating that the hole is part of this virtual manifold. Comparison of the molecular-orbital coefficients with the calculated total spin densities indicates that the oxygen *p*-spin density arises almost exclusively from a single-β-spin virtual orbital which we will call the "hole state." The energy level of this orbital is indicated in Fig. 4.

It should be noted that these "energy levels" are the Hartree-Fock parameters, and thus care must be exercised when interpreting them physically. If they are taken to be the real electronic energies, then the hole orbital is part of the conduction band. If the frozen-orbital approximation is carefully applied,<sup>28</sup> we find that the energy needed to promote an electron from the highest occupied state to the hole state is reduced from 10.5 to 1.7 eV. This large reduction in the energy difference arises from the inclusion of the appropriate Coulomb and exchange integrals in the energy difference<sup>28</sup>

$$E_{f,i} = \epsilon_f - \epsilon_i - \langle if || if \rangle . \quad (1)$$

TABLE I. *p*-spin density, in percent, on the peroxy radical. See Fig. 3 for site nomenclature.

	Density (%)		
O <sub>1</sub>	26	23	33
O <sub>2</sub>	74	77	67
Ref.	1	Theory—SPR	Theory—PR

TABLE II. Computed *s*-spin density on the silicon atoms of the peroxy radical (in arbitrary units). See Fig. 3 for site nomenclature.

	Density—SPR	Density—PR
Si <sub>1</sub>	1.00	1.00
Si <sub>2</sub>	0.57	0.0028

Here the  $\epsilon$ 's are the Hartree-Fock parameters,  $E_{f,i}$  is the energy difference between initial and final states, and  $\langle if || if \rangle$  is the difference between Coulomb and exchange integrals involving initial and final states.

It is important to note that this large energy reduction strengthens the analogy between free O<sub>2</sub><sup>-</sup> and the peroxy radical in SiO<sub>2</sub>. The highest occupied molecular orbital for free O<sub>2</sub><sup>-</sup> is one of the degenerate antibonding  $\pi$  orbitals. The lowest unoccupied molecular orbital is the other  $\pi$  orbital so that the energy difference is zero. The same argument should hold for the peroxy radical in SiO<sub>2</sub> with a slight modification. In this case the energy levels and wave functions are perturbed by the bonding between the peroxy and the SiO<sub>2</sub> network. The  $\pi$  orbitals are split as the symmetry is lowered

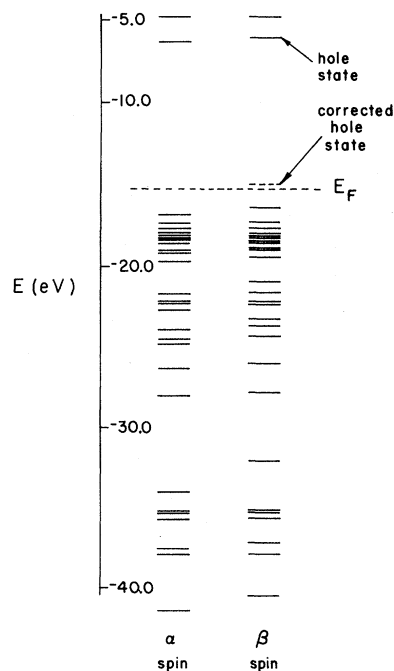


FIG. 4. Single-particle energy levels for the SPR, with  $\alpha$ -quartz geometrical constraints, as calculated using MOPN. All states below the dashed line are occupied. The hole state is indicated.

from  $D_h^\infty$  to approximately  $C_s$ . However, this splitting should not be very large if the perturbation picture is appropriate. By analyzing the wave-function coefficients of the highest occupied  $\beta$ -spin molecular orbital, we determined that it was predominantly oxygen  $2p$ , and that it pointed  $90^\circ$  away from the hole state and  $86.0^\circ$  away from the  $O_1$ - $O_2$  vector, consistent with the perturbed  $O_2^-$  picture.

The results shown in Table II for the SPR clearly indicate that while this may possibly be a stable defect, it is not the peroxy radical observed by Griscom and co-workers. While our  $^{29}\text{Si}$  hyperfine interaction is asymmetric, a 12:7 ratio would give a qualitatively different EPR spectrum than was obtained by Griscom *et al.*, who obtain a 5:1 ratio as a lower bound.<sup>3</sup> We thus see that although the existence of an inequality in the two  $^{29}\text{Si}$  hyperfine interactions does not disprove the SPR model, the observed magnitude of the inequality is inconsistent with that model.

We next performed a set of calculations relaxing the constraint that the outer oxygens be in  $\alpha$ -quartz positions. In these calculations we first set the silicon-silicon distance at values from 3.05 to 5.2 Å. The outer oxygen atoms were then set in tetrahedral coordination and were held fixed in each calculation. The hydrogen atoms were set 0.94 Å away from the outer oxygen to which each was bonded (the MINDO/3 equilibrium OH bond length) and the Si-O-H bond angles were set at  $144^\circ$ . Again, the cluster was given a net positive charge and the two silicon atoms and the two inner oxygen atoms were allowed to search for minima in total energy. We performed these calculations to find the minimum size of the oxygen cage that would lead to the observed asymmetry in both the  $^{17}\text{O}$  and  $^{29}\text{Si}$  hyperfine interactions.

Three qualitatively different physical situations were obtained. First, there was the SPR situation already discussed in which the  $O_1$  and  $O_2$  spin densities, and hence the  $^{17}\text{O}$  hyperfine interaction, were asymmetric, but the Si  $s$ -spin densities were more nearly symmetric than observed. Figure 3 shows a generic conformation that holds for this case. Such results were obtained for initial Si-Si separations less than 3.8 Å.

The second generic situation yielded symmetric  $^{17}\text{O}$  and  $^{29}\text{Si}$  hyperfine interactions. The conformation for this model is such that each of the two oxygen atoms is bonded to one of the silicon atoms. Such energy minima could be obtained over the entire range of initial Si-Si separation 3.05 to 5.2 Å, if the outer tetrahedra were suitably "twisted." This

is discussed later in connection with the peroxy precursor.

The third situation is the observed type, wherein both the  $^{17}\text{O}$  and the  $^{29}\text{Si}$  hyperfine interactions are asymmetric. The conformation is generally quite similar to Fig. 1(c). Such energy minima occur for initial Si-Si separation greater than 4.8 Å.

Note that the above discussion implies that the peroxy radical may have several local energy minima for a given outer oxygen "cage." The total energies will then dictate which conformation will dominate in various situations. The most important result is illustrated in Table III; namely, the peroxy-radical conformation leading to the observed hyperfine asymmetries is energetically favored only for initial Si-Si separations of 5.2 Å and larger.

While this Si-Si separation may seem unreasonably large, predictions of this size are not without precedent. To explain the anomalous low-temperature specific heat of  $\alpha$ - $\text{SiO}_2$ , the existence of two-level tunneling systems was postulated.<sup>29,30</sup> One particular microscopic model for these two level systems involves Si-O-Si linkages in which the oxygen atom is off center.<sup>31,32</sup> These off-center systems have a double-well potential surface, and motion between these wells is assumed to take place even at very low temperatures. Theoretical calculations<sup>31,33</sup> have been done to determine the Si-Si separation needed to induce the oxygen atom to move off center. A simple Morse potential calculation<sup>31</sup> predicted that the onset of this occurred at 3.8 Å, while calculations using MINDO/3 predicted<sup>33</sup> the onset would be at 4.2 Å. (Calculations on disiloxane using<sup>34</sup> Gaussian 76 at  $R_{\text{Si-Si}}=4.2$  Å predicted that the oxygen would not be far off center,  $R_{\text{Si-O}}=1.85$  Å, so that the MINDO/3 prediction can be considered reasonable.)

The calculated conformation of the asymmetric peroxy radical for an initial Si-Si separation of 5.2 Å is represented schematically in Fig. 5. Several

TABLE III. Computed heats of formation  $\Delta H_F$  for different initial Si-Si separations. Sym (nonsym) indicates that the local minimum energy configuration leads to symmetric (nonsymmetric)  $^{29}\text{Si}$  and  $^{17}\text{O}$  hyperfine interactions.

Initial $R_{\text{Si-Si}}$ (Å)	$\Delta H_F$ (sym) (eV)	$\Delta H_F$ (nonsym) (eV)
4.8	-19.92	-18.42
5.0	-18.97	-18.43
5.2	-18.44	-18.65

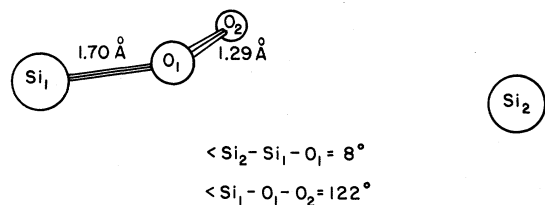


FIG. 5. Schematic representation of the calculated atomic positions for the peroxy radical for an initial Si-Si separation of 5.2 Å. Outer oxygens are omitted for convenience.

salient features of this calculation should be noted. The O<sub>1</sub>-O<sub>2</sub> bondlength is 1.29 Å, again very close to the experimental value for free O<sub>2</sub><sup>-</sup> (1.30 Å), and to the MOPN prediction (1.31 Å). The peroxy radical is clearly attached to a single silicon atom. In Table IV we list the resulting Si<sub>1,2</sub>-O<sub>1,2</sub> bond distances.

Not shown in Fig. 5 is the important feature that the threefold-coordinated silicon atom has relaxed almost completely back into the plane of the three neighboring oxygen atoms, while the silicon to which the peroxy radical is attached has remained in a tetrahedral configuration. The final Si-Si separation is 6.01 Å, indicative of the large relaxation that Si<sub>2</sub> underwent.

We now consider the electronic structure of the peroxy radical. In Table I we compare the calculated *p*-spin densities on the peroxy oxygen atoms to those predicted by Griscom *et al.* The asymmetry predicted by MOPN is in good agreement with experiment. We also include the silicon *s*-spin densities predicted by MOPN. These are shown in Table II. These spin densities imply that the ratio of hyperfine interaction between Si<sub>1</sub> and Si<sub>2</sub> is 480:1. This is consistent with the <sup>29</sup>Si data for the dry oxides.<sup>3</sup>

The single-particle eigenvalue spectrum for the PR is found to be similar to that of the SPR. As with the small R<sub>Si-Si</sub> cluster, the single-particle state associated with the hole is part of the conduction band. By making the appropriate correction to the excitation energies [using Eq. (1)], the energy difference between the highest occupied molecular orbital and the hole state is lowered from 10.34 to

TABLE IV. Computed distances between the silicon atoms and the peroxy oxygen atoms, in Å, for the PR with an initial Si<sub>1</sub>-Si<sub>2</sub> separation of 5.2 Å.

	O <sub>1</sub>	O <sub>2</sub>
Si <sub>1</sub>	1.71	2.63
Si <sub>2</sub>	4.23	3.90

0.01 eV. The hole eigenstate is again predominantly lone pair ( $\pi$ -like), and points 89.5° out of the Si<sub>2</sub>-O<sub>1</sub>-O<sub>2</sub> plane. Again, the picture of the peroxy radical as a perturbed O<sub>2</sub><sup>-</sup> ion suffices to explain both the experimental results and the theoretical calculations.

## B. The peroxy precursor

Using the same cluster, but with no charge, we performed calculations on the presumed peroxy precursor. We started with an  $\alpha$ -quartz oxygen cage, the same used in the first SPR calculation. Again, we allowed the two silicon atoms and the two central oxygen atoms to search for positions that minimized the total energy.

The equilibrium conformation of the computed SPR precursor is shown in Fig. 6. It is interesting to note that this precursor is not a linkage, but rather an oxygen atom trapped by a single bridging oxygen atom. This is also inferred by the interatomic distances shown in Table V. The heat of formation of this cluster is -25.8 eV. This should be compared to the heat of formation of the  $\alpha$ -quartz cluster with a single bridging oxygen, which is -29.5 eV. The difference between these two heats of formation has the following significance. The heats of formation calculated by MOPN compare the energies of infinitely separated atoms to the atoms bonded to form a molecule. The difference then implies that the second oxygen would prefer to be infinitely distant from the cluster by 3.7 eV. This difference can be used to calculate a Boltzmann factor that gives the ratio of double bridging oxygen atoms to single bridging oxygen atoms plus single oxygen atoms. (In this analysis we are neglecting the effect of the solid on a "free" interstitial oxygen atom. An improved scheme would be to calculate the total energy of a free oxygen atom and of an oxygen atom in

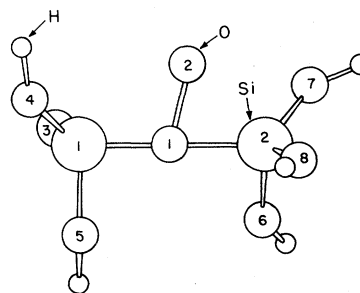


FIG. 6. Conformation of the peroxy precursor with outer oxygen atoms in  $\alpha$ -quartz positions.

TABLE V. Computed interatomic distances for the peroxy precursor, in Å, for the SPR.

	O <sub>1</sub>	O <sub>2</sub>
Si <sub>1</sub>	1.92	1.63
Si <sub>2</sub>	2.41	1.60

an appropriate crystal potential. The difference in these energies would be subtracted from 3.7 eV.) For 3.7 eV this ratio is about  $10^{-13}$  at 1200°C. So we predict that during the growth process the density of double oxygen atoms will be no more than about  $10^{10} \text{ cm}^{-3}$ , 6 orders of magnitude lower than the known experimental value for the density of peroxy radicals in the experiments of Griscom and co-workers.<sup>1-3</sup> This cannot be a precursor for the observed peroxy radicals.

In the case of large Si-Si separation, using, for instance, the same initial geometry as for the asymmetric peroxy radical, the opposite condition holds. A peroxy linkage is strongly favored over a single oxygen atom. This is not surprising, since with such a large Si-Si separation, a single oxygen atom is bonded to only one silicon atom,<sup>33</sup> leaving a bond dangling from the other silicon.

The minimum energy conformation for this case, with the initial Si-Si separation of 5.2 Å, is shown schematically in Fig. 7. Our calculation indicates that if the outer oxygen atoms are frozen, then, for the neutral cluster, the silicon outer oxygen bonds will stretch to about 1.69 Å, allowing the Si-Si separation to shrink from 5.2 to 4.84 Å, thus stabilizing the bonds between the silicon atoms and the peroxy linkage. The oxygen-oxygen separation for the peroxy linkage, 1.45 Å, is close to the MOPN prediction for the bond length for O<sub>2</sub><sup>2-</sup>.

For Si-Si separations between 3.05 and 4.2 Å, the relative stability of single and double bridging oxygen atoms depends on the orientation of the outer

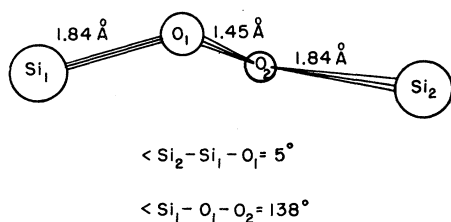


FIG. 7. Schematic representations of the calculated atomic positions for the peroxy precursor with initial Si-Si separation of 5.2 Å. Outer oxygen atoms are omitted for convenience.

oxygen atoms. We performed a set of calculations in which the silicon atoms were set at various distances from 3.05 to 4.2 Å. In these calculations the outer oxygen atoms were constrained to move rigidly in tetrahedral coordination, that is (with subscripts as in Fig. 6),

$$\begin{aligned} \angle \text{O}_4 - \text{Si}_1 - \text{O}_5 &= \angle \text{O}_4 - \text{Si}_1 - \text{O}_3 \\ &= \angle \text{O}_5 - \text{Si}_1 - \text{O}_3 = 109.47, \end{aligned}$$

in degrees, and

$$R_{\text{Si}_1 - \text{O}_{3-5}} = 1.63,$$

in Å.

Similar constraints were placed on O<sub>6-8</sub> and Si<sub>2</sub>. During the energy search, we required that

$$\begin{aligned} \angle \text{O}_4 - \text{Si}_1 - \text{O}_1 &= \angle \text{O}_5 - \text{Si}_1 - \text{O}_1 \\ &= \angle \text{O}_3 - \text{Si}_1 - \text{O}_1 = 109.47, \end{aligned}$$

$$\begin{aligned} \angle \text{O}_7 - \text{Si}_2 - \text{O}_2 &= \angle \text{O}_8 - \text{Si}_2 - \text{O}_2 \\ &= \angle \text{O}_6 - \text{Si}_2 - \text{O}_2 = 109.47, \end{aligned}$$

both in degrees, so that the outer oxygen atoms moved rigidly with O<sub>1</sub> and O<sub>2</sub>. The terminating hydrogen atoms were constrained to move rigidly with the outer oxygen atoms (Si-O-H angles were fixed at 144°). The silicon atoms were not allowed to relax for reasons discussed in Sec. III. A typical minimum energy conformation under these constraints is shown in Fig. 8.

After the minimum energy configuration was found, the outer oxygen and hydrogen atoms were fixed at these positions, one of the central oxygen atoms was removed, and the remaining central oxygen atom was allowed to relax. Under these conditions we found that there are cases for which a peroxy linkage is energetically favored over a single bridging oxygen atom. This is true for  $R_{\text{Si-Si}}$  as small as 3.17 Å. These, however, may well involve physically unrealistic positions for the outer atoms.

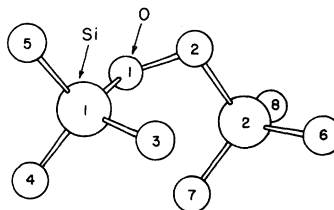


FIG. 8. Minimum energy configuration for peroxy precursor at  $R_{\text{Si-Si}} = 3.15 \text{ Å}$ .

## V. DEFECT FORMATION

As stated above, to explain the annealing data Friebele *et al.*<sup>2</sup> hypothesized that the peroxy precursor easily sheds an electron upon heating. We have not seen evidence for this in our calculations, as we predict the electrical level of the peroxy radical to be about 5.2 eV below the conduction-band edge. (Fig. 9). The energy difference between the relaxed PR precursor and the relaxed PR is computed to be 6.4 eV. This is the amount of energy needed to remove one electron from the cluster to infinity. A more realistic energy would be the amount needed to promote the electron to the conduction band. This can be estimated by subtracting the electron affinity<sup>35</sup> for SiO<sub>2</sub>, 1.2 eV, from the energy calculated above. The result, 5.2 eV, is still very large to surmount thermally.

There are other mechanisms, not included in our calculations, that could make it easier than we have predicted for the peroxy precursor to lose an electron. For example, we are allowing only four atoms to relax in our calculations, when in fact many may take part in the relaxation, thus increasing the lattice relaxation energy.

A second possibility is that the precursor captures a free hole, released from some shallow hole trap. Since annealing data (Fig. 2) indicate that the peroxy radical grows in over the same temperature range as the  $E'$  center anneals out, in an almost perfect one for one replacement of peroxy radicals for  $E'$  centers, we investigated the possibility that  $E'$  centers are the source of these holes. We calculated the electrical level of the  $E'$  center using the same method as we used for the peroxy radical. That is, for both the charged and uncharged cluster, we allowed both silicon atoms to relax inside the  $\alpha$ -quartz oxygen cage. (In the case of the neutral cluster, the equilibrium Si-Si distance was 2.84 Å, indicating that a strained Si-Si bond has formed.) The electrical level is then calculated by taking the difference in total energy between the charged cluster and the neutral cluster and subtracting the electron affinity. This level for the  $E'_1$  center is 5.4 eV

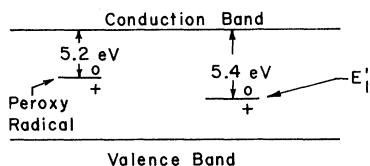


FIG. 9. Electrical levels for the peroxy radical and for the  $E'_1$  center as calculated using MOPN.

(Fig. 9). The  $E'$  level is shallower than that of the peroxy radical, but still is deep. Thus the transfer of holes from  $E'$  centers to peroxy precursors may be very slow. The rate could be enhanced by tunneling if the defects were sufficiently close to one another, but we have insufficient information to evaluate this possibility.

Hole-capture mechanisms have other interesting features. If Griscom's model of the NBOHC [Fig. 1(b)] is correct, this defect should capture a second hole and release a  $H^+$ . The central oxygens then represent a peroxy precursor, which can capture a hole and become a PR. This could account for the observed disappearance of the NBOHC while the PR grows, and in fact the behavior of the PR, NBOHC, and  $E'$  centers as shown in Fig. 2 are consistent with this suggestion, at least up to 300°C.

There is one problem with both electron shedding and hole trapping mechanisms. Our calculations imply that a large majority of precursor linkages will be too small to break apart when positively charged. We certainly overestimate the difficulty to break apart by having both "halves" of the precursor rather symmetric, certainly more so than in a real amorphous material. This could partially resolve the problem, but it seems unlikely that all the linkages will be sufficiently asymmetric to break apart when ionized. A further resolution of this problem is to assume that a peroxy linkage will not trap a hole unless it breaks apart. We thus envision peroxy sites which may affect the mobility of holes but not serve as hole traps.

There is a third possibility, an O<sub>2</sub> diffusion mechanism which we have considered in detail for the small peroxy radical. Recent experiments indicate that it might also obtain for the large (asymmetric) peroxy radical.<sup>3</sup> We suggest the following scenarios as a possibility for SPR formation:

(1) Initial irradiation creates oxygen vacancies, free oxygen atoms, and free electrons and holes. Some of these free oxygen atoms and holes are trapped by bridging oxygen atoms to form peroxy radicals.

(2) Holes are also trapped at oxygen vacancies to form  $E'$  centers. (There are other hole traps in the oxide, but they are not being considered here. The free electrons are also trapped, though the nature of these traps is not yet known.) Some of the oxygen atoms combine to form O<sub>2</sub>, which enhances the preexisting concentration of interstitial O<sub>2</sub>. Our calculations indicate that at temperatures at which the dissolved O<sub>2</sub> can diffuse,<sup>36</sup> these O<sub>2</sub> can then combine with  $E'$  centers<sup>37</sup> to form more stable

peroxy radicals. That the peroxy radical is more stable than the  $E'$  center is borne out by the annealing data and by our calculations.

We made some order-of-magnitude estimates of the capture rate of  $O_2$  molecules by  $E'$  centers to see if there were any obvious flaws in the diffusion model for peroxy formation. We used the standard result from Waite<sup>38</sup> for bimolecular reaction rates in solids:

$$\frac{dC_{E'}}{dt} = \frac{dC_{O_2}}{dt} = -4\pi r^* DC_{E'} C_{O_2} \left[ 1 + \frac{r^*}{(\pi Dt)^{1/2}} \right], \quad (2)$$

where  $C_{E'}$  and  $C_{O_2}$  are the concentrations of  $E'$  centers and of interstitial oxygen molecules,  $D$  is the diffusion coefficient for  $O_2$ , and  $r^*$  is a capture radius. Equation (2) is valid for diffusion-limited processes for which there is no activation energy for the reaction.

Several papers on oxygen diffusion through fused silica have appeared in the literature.<sup>39-43</sup> The diffusion coefficient  $D$  is written in the form

$$D = A \exp(-E/kT). \quad (3)$$

While there is reasonable agreement as to the size of

$$C_{E'} = \frac{(C_{E'}^0 - C_{O_2}^0) C_{E'}^0}{C_{E'}^0 - C_{O_2}^0 \exp \left[ -4\pi r^* D (C_{E'}^0 - C_{O_2}^0) \left[ 1 + \frac{2r^*}{(\pi Dt)^{1/2}} \right] t \right]}. \quad (4)$$

We estimated the capture radius to be 5 Å, approximately the lattice constant. The values for the initial concentrations  $C_{E'}^0$  and  $C_{O_2}^0$  were<sup>43</sup>  $2.0 \times 10^{16} \text{ cm}^{-3}$  and  $6.2 \times 10^{16} \text{ cm}^{-3}$ , respectively. The results are given in Fig. 10.

These results indicate that as a result of the  $O_2$  diffusion mechanism, the  $E'$  center concentration should fall off rapidly in the (250–300)°C range, which is considerably higher than the temperature (~200°C) at which the observed falloff occurs. This is evident by comparing Figs. 2 and 10. Only if the initial concentration of  $O_2$  were several orders of magnitude larger or if the activation energy for diffusion were smaller could this mechanism account for the observed decrease in the number of  $E'$  centers.

The  $O_2$  diffusion mechanism could be tested experimentally. If isochronal pulse annealing studies were performed in an atmosphere of very high and

TABLE VI. Values for pre-exponential factor  $A$  and for activation energy  $E$  for  $O_2$  diffusion in fused silica.

$A$ ( $\text{cm}^2/\text{sec}$ )	$E$ (eV)	Ref.
$2.88 \times 10^{-4}$	1.17	43
$2.0 \times 10^{-9}$	1.26	40
$4.0 \times 10^{-11}$	0.85	41

the activation energy  $E$ , values for the pre-exponential factor,  $A$ , vary by as much as 5 orders of magnitude. The various values of  $E$  and  $A$  are given in Table VI. The first set of values in Table VI, due to Norton, were obtained from a straightforward permeability experiment, while the latter two sets were the result of isotope exchange experiments.

The difference between Norton's and Williams's results was lucidly discussed by Meek,<sup>39</sup> who showed that Williams actually measured permeability, not diffusion. Meek's argument, coupled with the fact that Norton's result agrees well with data on oxidation of silicon,<sup>44</sup> led us to use Norton's coefficient for our present discussion.

Equation (2) is analytically integrable, yielding

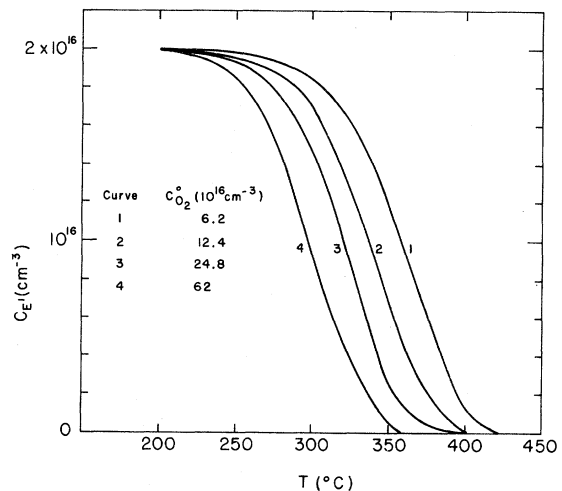


FIG. 10. Plot of  $E'$  concentration  $C_{E'}$ , vs temperature for several different initial concentrations of  $O_2$  ( $C_{O_2}^0$ ), from Eq. (4). Other parameters are as given in text.

very low O<sub>2</sub> pressure, the temperature at which the annihilation of  $E'$  centers occurs should increase and decrease, respectively. As shown in Fig. 10, if the density of O<sub>2</sub> increases by an order of magnitude, the annealing curve moves by about 50°C.  $\alpha$ -quartz may, for the following reasons, be a good material on which to attempt this experiment. Our calculations indicate that peroxy precursors are highly unlikely to occur in  $\alpha$ -quartz. We also have a good idea of the structure of the  $E'_1$  center in this material. Finally, because of the large  $c$ -axis channels in  $\alpha$ -quartz, O<sub>2</sub> diffusion probably occurs rather easily.

## VI. SUMMARY

To summarize, we have demonstrated that the peroxy-radical model proposed by Griscom and co-workers is consistent with theoretical calculations. These calculations have placed constraints on the local geometry of the peroxy radical and precursor. They have demonstrated that large silicon-silicon separations are needed for the peroxy linkage to be preferred to a single bridging oxygen atom, unless the neighboring Si-O tetrahedra are considerably twisted. They have also demonstrated that with

large Si-Si separations, the radical will trap on one of the silicon atoms with a large accompanying lattice relaxation. Finally, we have suggested a second possible model for the observed peroxy radical, the SPR. A formation mechanism for this defect has been proposed. This mechanism is directly testable via experiments which we have suggested.

## ACKNOWLEDGMENTS

The authors thank Dr. D. L. Griscom and Dr. E. J. Friebele for introducing us to the problem of the peroxy radical, for several useful discussions and for showing us their <sup>29</sup>Si hyperfine results prior to publication. Valuable comments were made by Dr. G. D. Watkins, Dr. F. J. Feigl, Dr. S. R. Butler, and Arun Chatterjee. We also thank the staffs of the Lehigh University Computing Center, and of the Brookhaven National Laboratory Computing Facility for their help with the computational aspects of this work, and the Lehigh Computing Center for the considerable free computer time which was supplied. The Quantum Chemistry Program Exchange supplied computer programs used in this work. This research was supported by the Office of Naval Research under Contract No. N00014-76-C-0125.

- 
- <sup>1</sup>M. Stapelbroek, D. L. Griscom, E. J. Friebele, and G. H. Sigel, Jr., *J. Non-Cryst. Solids* **32**, 313 (1979).  
<sup>2</sup>E. J. Friebele, D. L. Griscom, M. Stapelbroek, and R. A. Weeks, *Phys. Rev. Lett.* **42**, 1346 (1979).  
<sup>3</sup>D. L. Griscom and E. J. Friebele, *Phys. Rev. B* **24**, 4896 (1981).  
<sup>4</sup>D. L. Griscom, E. J. Friebele, and G. H. Sigel, *Solid State Commun.* **15**, 479 (1974); D. L. Griscom, *Phys. Rev. B* **20**, 1823 (1979).  
<sup>5</sup>D. L. Griscom, *Phys. Rev. B* **22**, 4192 (1980).  
<sup>6</sup>These charge assignments are consistent with the ionic picture of SiO<sub>2</sub> [Si<sup>4+</sup>(O<sup>2-</sup>)<sub>2</sub>]. They can be regarded as a mere bookkeeping convenience, and do not imply that SiO<sub>2</sub> is in fact ionic.  
<sup>7</sup>F. J. Feigl, W. B. Fowler, and K. L. Yip, *Solid State Commun.* **14**, 225 (1974); K. L. Yip and W. Beall Fowler, *Phys. Rev. B* **11**, 2327 (1975).  
<sup>8</sup>Exploratory one-electron calculations on this defect have been recently completed [E. O'Reilly and J. Robertson (unpublished)].  
<sup>9</sup>A. Edwards and W. B. Fowler (unpublished).  
<sup>10</sup>R. A. Weeks, *J. Appl. Phys.* **27**, 1376 (1956). Weeks has subsequently discussed possible peroxy models associated with such defects [see, e.g., R. A. Weeks, in *Interaction of Radiation with Solids*, edited by A. Bishay (Plenum, New York, 1967), p. 55].  
<sup>11</sup>Robert H. Silsbee, *J. Appl. Phys.* **32**, 1459 (1961).  
<sup>12</sup>R. A. Weeks and C. M. Nelson, *J. Am. Ceram. Soc.* **43**, 399 (1960).  
<sup>13</sup>D. L. Griscom, in *Defects and Their Structure in Nonmetallic Solids*, edited by B. Henderson and A. E. Hughes (Plenum, New York, 1976), p. 323.  
<sup>14</sup>E. J. Friebele, D. L. Griscom, and G. H. Sigel, Jr., in *The Physics of Non-Crystalline Solids*, edited by G. H. Frischat, (Trans Tech Publications, Aedermannsdorf, Switzerland, 1977), pp. 154–159.  
<sup>15</sup>Sigmund Urnes, *Trans. Brit. Ceram. Soc.* **60**, 85 (1961).  
<sup>16</sup>H. R. Zeller and W. Kanzig, *Helv. Phys. Acta* **40**, 845 (1967).  
<sup>17</sup>J. O. Edwards, D. L. Griscom, R. B. Jones, K. L. Waters, and R. A. Weeks, *J. Am. Chem. Soc.* **91**, 1095 (1969).  
<sup>18</sup>P. Bischof, *J. Am. Chem. Soc.* **98**, 6844 (1976).  
<sup>19</sup>Richard C. Bingham, Michael J. S. Dewar, and Donald H. Lo, *J. Am. Chem. Soc.* **97**, 1285 (1975).  
<sup>20</sup>M. J. S. Dewar, D. H. Lo, and C. A. Ramsden, *J. Am. Chem. Soc.* **97**, 1311 (1975).  
<sup>21</sup>S. DeBruijn, *Chem. Phys. Lett.* **54**, 399 (1978).  
<sup>22</sup>J. A. Pople, *J. Am. Chem. Soc.* **97**, 5306 (1975).  
<sup>23</sup>L. A. Burke, G. Leroy and M. Sana, *Theor. Chim.*

- Acta **40**, 313 (1975).
- <sup>24</sup>R. J. Bell and P. Dean, *Philos. Mag.* **25**, 1381 (1972).
- <sup>25</sup>M. O'Keeffe and B. G. Hyde, *Acta Cryst. B* **34**, 27 (1976).
- <sup>26</sup>Oak Ridge Thermal Ellipsoid Plotting Routine.
- <sup>27</sup>D. R. Stull and H. Prophet, *Janaf Thermochemical Tables*, 2nd ed. (National Bureau of Standards, Washington D.C., 1971).
- <sup>28</sup>D. Firsht, B. T. Pickup, and R. McWeeney, *Chem. Phys.* **29**, 67 (1978).
- <sup>29</sup>P. W. Anderson, B. I. Halperin, and C. Varma, *Philos. Mag.* **25**, 1 (1972).
- <sup>30</sup>W. A. Phillips, *J. Low Temp. Phys.* **7**, 351 (1972).
- <sup>31</sup>R. E. Strakna, *Phys. Rev.* **123**, 2020 (1961).
- <sup>32</sup>C. Laermans, *Phys. Rev. Lett.* **42**, 250 (1979).
- <sup>33</sup>W. B. Fowler and A. H. Edwards, in *The Physics of MOS Insulators*, edited by S. Pantelides and F. L. Galeener (Pergamon, New York, 1980), pp. 59; A. H. Edwards (unpublished).
- <sup>34</sup>Gaussian 76 is an *ab initio* LCAO-MO program, obtained from the Quantum Chemistry Program Exchange.
- <sup>35</sup>D. L. Griscom, *J. Non-Cryst. Solids* **24**, 155 (1977).
- <sup>36</sup>Most researchers agree that oxygen diffuses as O<sub>2</sub> in SiO<sub>2</sub>.<sup>39-43</sup> The low activation energy, combined with experimental evidence<sup>45</sup> that oxygen diffuses without isotope exchange, indicates that there is no bond breaking associated with its motion. It is then similar to a rare-gas atom. It is interesting to note, as Meek<sup>39</sup> did, that argon and oxygen have almost identical diffusion activation energies and molecular radii<sup>46,47</sup> in SiO<sub>2</sub>. The preexponential factors for Ar and O<sub>2</sub>, obtained from permeability experiments,<sup>43,46</sup> differ by only a factor of 2;  $D_0 = 1.21 \times 10^{-4}$  cm<sup>2</sup>/sec for Ar and  $2.88 \times 10^{-4}$  cm<sup>2</sup>/sec for O<sub>2</sub>.
- <sup>37</sup>A similar, though not identical, model has been suggested by Greaves [G. N. Greaves, *Philos. Mag. B* **37**, 447 (1978)].
- <sup>38</sup>T. R. Waite, *Phys. Rev.* **107**, 463 (1957).
- <sup>39</sup>Ronald L. Meek, *J. Am. Ceram. Soc.* **56**, 341 (1973).
- <sup>40</sup>E. L. Williams, *J. Am. Ceram. Soc.* **48**, 190 (1965).
- <sup>41</sup>K. Muehlenbachs and H. A. Schaeffer, *Can. Mineral.* **15**, 179 (1977).
- <sup>42</sup>Eugene Sucov, *J. Am. Ceram. Soc.* **46**, 14 (1963).
- <sup>43</sup>F. Norton, *Nature* **191**, 701 (1961).
- <sup>44</sup>B. E. Deal and A. S. Grove, *J. Appl. Phys.* **36**, 3370 (1965).
- <sup>45</sup>E. Rosencher, A. Straboni, S. Rigo, and G. Amsel, *Appl. Phys. Lett.* **34**, 254 (1979).
- <sup>46</sup>W. G. Perkins and D. R. Begeal, *J. Chem. Phys.* **54**, 1683 (1971).
- <sup>47</sup>J. F. Lee, F. W. Sears, and D. L. Turcoates, *Statistical Thermodynamics* (Addison Wesley, Reading, Mass., 1963), p. 82.